

which can ultimately reduce the system capacity. Hence, hardware design becomes a challenging and complicated process while efficient adaptive algorithms applied in software become a preferable choice to develop effective self-interference mitigation techniques.

A power allocation strategy is an example of using adaptive algorithms to mitigate the effect of self-interference. In optimum power allocation, the CSI is known at the transmitter. The CSI information can be used to obtain the singular value decomposition (SVD) to identify effective independent channels. The singular values are used as decision criteria to determine the power allocation such that parallel spatial channels corresponding to higher singular values are assigned more power, while no power is allocated to the spatial interferer resulting from the low singular values due to high correlation.

Ivral *et al.* [16] introduced an adaptive algorithm, by combining antenna selection and power allocation strategy in highly correlated channels. Instead of using the CSI as the feedback information, the correlation matrix is used as the performance metric as it is shown that correlation matrix overhead is much less compared to eigenvalues from the SVD method, resulting in lower feedback requirements and thus a faster allocation process. From the correlation matrix, the transmitter applies stochastic water-filling power allocation to get the maximum capacity from the correlated channels. However, achieving optimal bit assignment becomes the main challenge to realise the water-filling allocation, since modulation techniques are discrete and water-filling requires continuous bit allocation to substreams, with more bits transmitted to the dominant eigenmodes. This can be overcome by implementing adaptive modulation and coding scheme.

Another antenna selection strategy is proposed by Gore *et al.* [17]. The algorithm chooses the optimum subset of transmit and receive antennas based on minimum symbol error rate. It was proven that the selection algorithm enhanced the SM performance in correlated environments, but at the expense of a loss in data rate.

Akhtar and Gesbert [18] proposed the use of constellation multiplexing (CM) to minimise spatial interference. The main key in CM transmission is from the use of power scaling, which is achieved by scaling down the desired M-QAM constellation size by the scaling factor from the original M-QAM size. Spatial subchannels are differentiated through power scaling rather than through spatial signature which is used in conventional SM transmission. For

example in a fully correlated channel, a 16-QAM signal is the superposition of two 4-QAM constellation signals, with the second 4-QAM constellation points being centred at the constellation point of the first 4-QAM points, as shown in Fig. 2. CM requires only a single transmit antenna to send several independent data streams from a given modulation scheme, provided it is power-scaled to form a higher-order modulation constellation. By transmitting in such manner, CM does not rely on a full rank channel matrix to function properly. Hence, such schemes yield a rate-preserving MIMO multiplexing scheme that can operate robustly at any degree of spatial correlation.

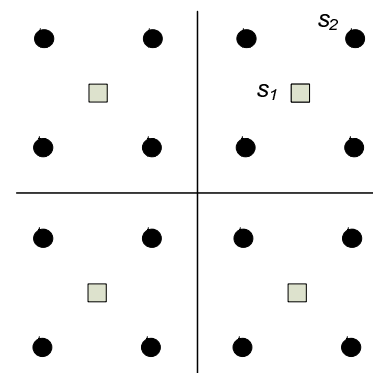


Fig. 2: Two superposed 4-QAM constellations, s_1 and s_2 that yields the equivalent 16-QAM constellations after scaled down by power of $\frac{1}{4}$ [18].

3 Self-Interference Mitigation Strategy

3.2 SINR Metric

In this section, a mathematical definition of the SINR metric is presented. SINR metric has knowledge of the channel quality at every subcarrier level, whereby it indicates the spatial information and self-interference caused by the mismatch between the spatial subchannels. The mathematical model for the received signal in a SM-OFDMA system, after FFT and guard removal is described as follows:

$$Y_u^s = H_u^s X_t^s + N_u^s \quad (3)$$

where the subscript u denotes the MS index, s denotes the subcarrier index, H_u^s is the channel matrix containing MS u 's frequency responses of the channels between N_t transmit and N_r receive

antennas at subcarrier s and applied to the subcarriers of the OFDMA signal on a cluster basis, while N_u^s denotes AWGN noise and X_t^s denotes $N_t \times 1$ matrix containing transmit signals. At the receiver, the OFDMA system adopts a linear MMSE configuration:

$$G_u^s = \left((H_u^s)^H H_u^s + SNR^{-1} I \right) (H_u^s)^{-1} \quad (4)$$

The MMSE filter has the ability to mitigate self-interference whilst not adversely amplifying the received noise. The MMSE filter is also able to separate the spatial subchannels of the SM structure [19]. As a result, different spatial subchannels can be allocated to different users to achieve additional spatial multiuser diversity gain. On the other hand, this typically increases the amount of feedback by the number of spatial subchannels. The received signal is multiplied by an MMSE filter given by Eq.(4):

$$G_u^s Y_u^s = G_u^s Y_u^s X_t^s + G_u^s N_u^s \quad (5)$$

The receiver then calculates the SINR per subcarrier and feeds back that information to the transmitter. The SINR metric captures the variation of the self-interference within the frequency domain. The MS u computes the SINR at every spatial subchannel for every subcarrier [19] (the subcarrier index, s , is omitted for simplicity of presentation):

$$ESINR_u^q = \frac{\left| (G_u H_u)_{qq} \right|^2 \varepsilon_s}{\left| (G_u H_u)_{qj, j \neq q} \right|^2 \varepsilon_s + \left(|G_u|_{qq}^2 + \sum_{j \neq q} |G_u|_{qj}^2 \right) N} \quad (6)$$

where q is the spatial subchannel considered in the allocation algorithm. In the case of SISO system, $q = Q = N_r = 1$. ε_s denotes the average symbol energy and $| \cdot |_{qj}$ denotes the element located in row q and column j . The SINR metric aims to compute self-interference with knowledge from the data stream component, $| \cdot |_{qq}$ and self-interference component, $| \cdot |_{qj, j \neq q}$ from the adjacent transmitted data streams, also known as *spatial interferer*.

3.3 Interference-Aware Subcarrier Allocation Scheme

In OFDMA systems, with users fading independently, there is likely to be a user with a good channel at any given time slot or sub-carrier. By scheduling transmission so that users transmit at times and frequency resources when their channel

conditions are favourable, significant gains from the effective channel can be achieved.

If a deterministic rather than random allocation of subcarriers is employed, the multiuser diversity can be exploited to ensure most users can be allocated the best subcarriers for them with minimal clashes. As a result, system capacity can be maximized by always serving the user with the strongest channel and the capacity can be increased as the number of users is increased.

Initially, DSA work has focussed on SISO systems [20]. Subsequently, the research focus has been expanded to MIMO schemes by Y. Peng [21], whereby several variations of the algorithm (referred to as ‘schemes’) were introduced. Each scheme corresponds to different spatial correlation condition. Channel gain was used as a metric to determine the subcarrier allocation process. The first scheme, referred to here as DSA-Scheme 1, performed subcarrier allocation separately for each spatial subchannel and it takes no consideration of self-interference and relation of one spatial subchannel to the other adjacent subchannel.

An extension to DSA-Scheme 1, known as DSA-Scheme 5 aims to combat the effect of self-interference in a correlated environment. This scheme considers the previously allocated subcarriers from the previous spatial subchannel by means of iteration. The number of near adjacent subcarriers avoided is measured by parameter l . From the simulation results, it is shown that when $l=10$, significantly enhanced BER gain can be obtained in extremely correlated environments.

The proposed interference-aware subcarrier allocation scheme can be illustrated in Fig. 3. Instead of using the channel gain as the performance metric, the allocation scheme uses two different performance metrics to determine the subcarrier allocation at each of the spatial subchannels: (i) at the parallel subchannels, ESINR metric is used to identify the subcarriers that are affected by self-interference, and (ii) the spatial interferers use the channel gain as a metric to determine the subcarrier allocation.

The subcarrier allocation is applied independently across spatial subchannels. By doing the allocations in this manner, users are prevented from sharing the subcarriers with the spatial interferer, thus helping to avoid the use of an extra coding scheme and reducing the complexity of the algorithm. The combination of different performance metrics in the proposed subcarrier allocation is expected to reduce the effect of self-interference, whilst still seeking a maximal allocation of channel energy.

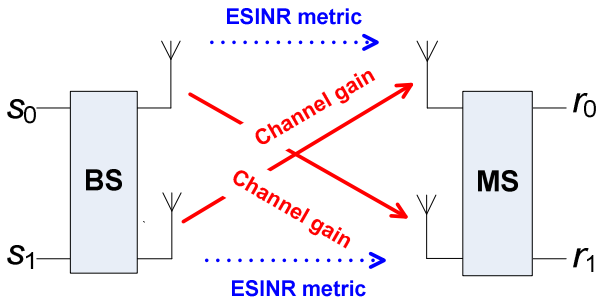


Fig. 1: Performance metric of the proposed interference-aware subcarrier allocation

This also ensures that spatial diversity cannot be lost due to highly correlated spatial subchannels since each of the spatial subchannels will be allocated with different sets of subcarriers.

Before the allocation takes place, the u -th MS computes the MMSE filter, (4), and multiplies the received signal by G_k , (5). The u -th mobile station then computes the SINR, of the q -th spatial subchannel, (6). The u -th MS calculates each SINR metric for each spatial subchannel and then sends them back through the feedback channel to the base station. The base station uses the feedback information as an input for the allocation algorithm.

The nomenclatures are set first as references. In the following algorithm, $q=\{1,\dots,Q\}$ represents spatial subchannel considered for the allocation algorithm. P_u^q and E_u^q represents the average received power gain and ESINR metric for user u at q^{th} spatial subchannel, U is the total number of users, S is an Q by N_q matrix where each row is a vector containing the indices of the useable subcarriers for the particular spatial subchannel, i.e. $N_q=\{1,\dots,N_{\text{sub}}\}$ where N_{sub} is the total number of useable subcarriers. The $h_{u,s}^q$ and $\text{SINR}_{k,s}^q$ is the channel response and ESINR metric for user u at subcarrier s and spatial subchannel q and $C_{s,u}$ is a matrix to store the subcarrier indices (subcarrier location) of the allocated subcarriers for user u and subcarrier s .

The interference-aware subcarrier allocation algorithm can be described as follow:

- (1) Initialization
Set $P_{u,q}=0$ for all users, $u=1,\dots,U$; Set $C_{u,s,q}=0$ for all users $u=1,\dots,U$ and spatial subchannel $q=\{1,2,\dots,Q\}$; Set $s=1$
- (2) Main process
While $N_q \neq 0_{N_{\text{sub}}}$

- (a.) Generate short list of users start with user with small SINR metric¹ and channel gain. Find user u satisfying:

$$\left. \begin{array}{l} \text{Main: } E_u^q \leq E_i^q \\ \text{Interferer: } P_u^q \leq P_i^q \end{array} \right\} \text{ for all } i, 1 \leq i \leq U$$
- (b.) For the user u in (a), find subcarrier s satisfying:

$$\left. \begin{array}{l} \text{Main: } \text{SINR}_{u,s}^q \geq \text{SINR}_{u,j}^q \\ \text{Interferer: } |h_{u,s}^q| \geq |h_{j,s}^q| \end{array} \right\} \text{ for all } j \in S$$
- (c.) Update $\text{SINR}_{u,s}^q$, P_u^q , N_q and $C_{s,u}$ with u and s in (b) according to:

$$E_u^q = E_u^q + \text{SINR}_{u,s}^q \quad (\text{for main spatial subchannel})$$

$$P_u^q = P_u^q + |h_{u,s}^q|^2 \quad (\text{for interferer channel})$$

$$N_q = N_q - n$$

$$C_{s,u} = n$$

$$s = s + 1$$
 where $C_{s,u}$ is the allocation matrix to record the allocated subcarrier, s for user u .
- (d.) Go to the next user in the short list in (a), repeat (b) to (c) until all users are allocated another subcarrier, $N_q \neq 0$. }

The algorithm ranks users from the lowest to highest SINR metric at each main spatial subchannel. Consequently, the next best subcarriers are allocated to users in rank order, allowing users with lowest SINR, i.e. users that suffer from ‘severe’ self-interference effect or poor received signal at that particular spatial subchannel to have the next best subcarrier with highest SINR metric that is available for the next transmission.

4 Simulation Environment

4.1 SM-OFDMA Design Parameters

The simulation is performed in an SM-OFDMA downlink environment. Modulation type affects both the data capacity in a given channel as well as the robustness with regard to noise and interference. The OFDM parameters and the considered Quadrature Phase Shift Keying (QPSK), $\frac{1}{2}$ rate modulation and coding scheme (MCS) are summarised in Table 1 and Table 2 and used throughout this paper.

¹ For the first iteration, assume all users have equal SINR metric as no subcarriers have been allocated; hence, the list may be entirely arbitrary.

Table 1: Physical layer parameter for OFDM system

Parameter	Value
Operating Frequency	5 GHz
Available Bandwidth (BW)	100 MHz
Transmit Information Duration (T_{tx})	10 ns
FFT size (N_{FFT})	1024
Useable subcarriers (N_{sub})	768
Subcarrier spacing (Δ_f)	97.66 kHz
Useful Symbol duration (T)	10.24 μ s
Guard Interval (GI)	176
Total Symbol Duration (T_s)	12.00 μ s

Table 2: QPSK, $\frac{1}{2}$ rate modulation scheme for the considered SM-OFDMA system

Modulation	QPSK
Coding Rate	$\frac{1}{2}$
Data bits per OFDM symbol	1536
Coded bits per OFDM symbol	3072
Total Bit per OFDM symbol	2048
Nominal Bit Rate [Mbps]	128
Total Bit Rate [Mbps]	170.67

The ideal wireless networks are characterised by their ability to operate in low SNR conditions but still offering high capacity with efficient spectrum utilisation. Therefore, suitable channel models are proposed to investigate the appropriate system. Both of the channels are adopted from two standards: (1) ETSI BRAN 'Channel E' [22] and (2) SCM 'Urban Micro' [23].

'Channel E' corresponds to a pico-cell type large open space environment with NLOS conditions, while 'Urban Micro' environment represents a very small cell in an ultra high density urban area with cell radius of approximately less than 500m and BS antennas located at rooftop level.

The MIMO channel models are simulated in a fixed channel matrix so that both receiver and transmitter are static with respect to each other and the path loss remains approximately constant during the measurement duration. Other than that, both channel models represent different multipath environments with different transmission bandwidths, which is relevant for comparison purposes in the simulation work throughout this paper. The key parameters for both channel models are summarised in Table 3.

A packet size of 54 bytes is considered throughout this paper. In addition to that, 2000 i.i.d quasi-static Rayleigh distributed channel samples per OFDM symbol are used in each simulation to

Table 3: Channel Models Parameters

Parameters	HIPERLAN 'E'	SCM Urban Micro
Environment	Large open space NLOS	Outdoor urban NLOS
Bandwidth	100 MHz	5 MHz
Excess Delay Spread	1760 ns	923 ns
Mean Delay Spread	250 ns	251 ns
Carrier Frequency	5 GHz	2 GHz

achieve stable averaging over wide fading channel. 16 users are considered to exploit the multiuser diversity gain with a total of 768 useable subcarriers to be equally shared among the users with FFT size, $N_{FFT}=1024$. A 2×2 antenna configuration is used for the SM scheme. It is assumed that the BS has perfect knowledge of the channel transfer function for those subcarriers that have been allocated to it and this is later used for equalisation and decoding purposes.

4.2 Correlation Coefficient

The spatial correlation matrix of the MIMO channel can be derived from the Kronecker model [8], a well-known correlation analytical model. Spatial correlation matrices between BS and MS, are given by:

$$\mathbf{R}_{MIMO} = \mathbf{R}_{MS} \otimes \mathbf{R}_{BS} \quad (7)$$

where \otimes represents the Kronecker product, and \mathbf{R}_{MS} and \mathbf{R}_{BS} are $N_r \times N_r$ and $N_t \times N_t$ matrices corresponding to transmit and receive covariance matrices, which can be further defined as symmetrical complex correlation matrices as follows:

$$\mathbf{R}_{BS} = \begin{bmatrix} \rho_{11}^{(z)} & \rho_{12}^{(z)} & \cdots & \rho_{1N_t}^{(z)} \\ \rho_{21}^{(z)} & \rho_{22}^{(z)} & \cdots & \rho_{2N_t}^{(z)} \\ \vdots & \vdots & \ddots & \vdots \\ \rho_{N_t 1}^{(z)} & \rho_{N_t 2}^{(z)} & \cdots & \rho_{N_t N_t}^{(z)} \end{bmatrix}_{N_t \times N_t} \quad (8)$$

$$\mathbf{R}_{MS} = \begin{bmatrix} \rho_{11}^{(z)} & \rho_{12}^{(z)} & \cdots & \rho_{1N_r}^{(z)} \\ \rho_{21}^{(z)} & \rho_{22}^{(z)} & \cdots & \rho_{2N_r}^{(z)} \\ \vdots & \vdots & \ddots & \vdots \\ \rho_{N_r 1}^{(z)} & \rho_{N_r 2}^{(z)} & \cdots & \rho_{N_r N_r}^{(z)} \end{bmatrix}_{N_r \times N_r} \quad (9)$$

where $\rho_{ij}^{(z)}$ is the transmission correlation coefficient:

$$\rho_{ij}^{(z)} = \left\langle \left| h_{N_t N_r}^{(z)} \right|^2, \left| h_{N_t N_r}^{(z)} \right|^2 \right\rangle \quad (10)$$

where $0 \leq \rho_{ij} \leq 1$ and $\langle a, b \rangle$ computes the correlation coefficient between a and b . Equation (7) assumes that the receive and transmit antenna are correlated independently on each other and assumes there are local scatterers near both antenna elements.

The Kronecker model allows separate optimisation at both link ends, so that receive and transmit correlations can be dealt with separately since the correlation properties at both transmit and receive antennas are independent from each other. Results published in [24] shown that Kronecker model is physically reasonable to use when the correlation between the adjacent antennas is larger than the correlation between non-adjacent antennas.

4.3 Correlated Channel Model

The main aim of this paper is to investigate the SM performance at different levels of spatial correlation: between ideal to extreme correlation scenario. In the ideal case, the channel is uncorrelated and the effect of self-interference is very minimal, while ‘fully’ correlated channel represents the worst case scenario, whereby the effective capacity gain is equal to a SISO system. The proposed correlation scenarios as summarised in Table 4. The correlation cases are derived based on practical wireless channel measurements from previous works as published in [25], [26] and [27].

Table 4: Correlation Modes and Its Coefficient

Correlation Modes	Correlation Coefficient, R_{MIMO}	
	R_{BS}	R_{MS}
‘Full’	0.99	0.99
Uncorrelated	0.00	0.00

Fig. 4 shows all the spatial subchannels in the uncorrelated 2x2 MIMO channel. It is observed that each spatial subchannel is randomly distributed across the subcarriers, which suggests that there is negligible influence from the other transmitting spatial subchannel (interferer) during the transmission. Fig. 5 is the example of the channel gain when it suffers from ‘fully’ correlated channel. It can be observed that the spectral shape and amplitude of channel gain at every spatial subchannel is almost identical. This is when the effect of self-interference dominates the MIMO performance and the effective channel is similar to SISO.

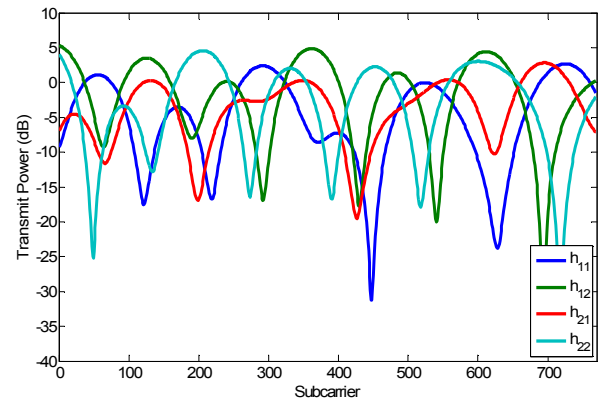


Fig. 2: Example of uncorrelated channel at every spatial subchannel for SCM ‘Urban Micro’

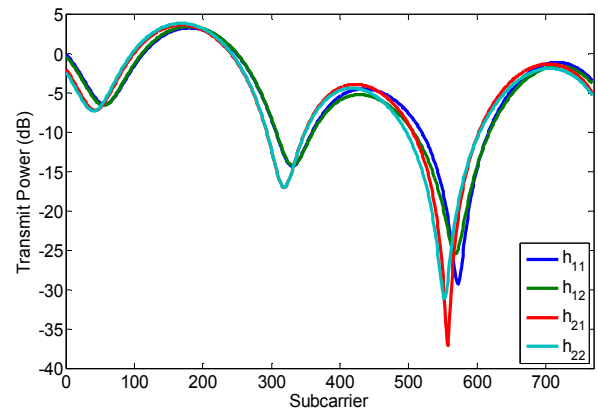


Fig. 3: Example of ‘Fully’ correlated channel at every spatial subchannel for SCM ‘Urban Micro’

5 Simulation Results

In Fig. 6, the performance of the proposed interference-aware subcarrier allocation is compared against DSA-Scheme 1 and DSA-Scheme 5, described earlier in Section 3.3. From the results, it is shown that the interference-aware allocation has better advantage in terms of BER gain, compared to DSA-Scheme 1 and DSA-Scheme 5 when simulated in both uncorrelated channel.

This result also suggests that the uncorrelated channel model carries some degree of self-interference, resulting in loss of BER gain. This can be confirmed from the measurement of correlation coefficient, R_{MIMO} between the parallel channel and the spatial interferer of the generated channel models (Table 5). The correlation coefficients for both channel models are considered as moderate number, thus acceptable in practical implementation as a MIMO channel is expected to generate some amount of spatial correlation, especially in a populated urban environment

Table 5: Correlation coefficient measurement for uncorrelated channel

Channel Model	Correlation Coefficient, R_{MIMO}	
	R_{BS}	R_{MS}
ETSI	0.224	0.276
SCM	0.446	0.320

In Fig. 7, the performance of the proposed interference-aware subcarrier allocation scheme is compared against DSA-Scheme 1 and DSA-Scheme 5 in a ‘Fully’ correlated channel environment. From the result, the benefit of interference-aware allocation is apparent in a fully correlated channel. In both channel models, the interference-aware allocation scheme shares almost similar BER performance to that of the DSA-Scheme 5. The margin of BER difference is increased significantly as the SNR increases, particularly beyond 10 dB, which implies the ability of interference-aware allocation to minimise self-interference in a highly correlated channel, while DSA-Scheme 5 suffers from propagation error as the SNR increases. DSA-Scheme 5 performance is also achieved an error floor as the SNR increase when simulated in uncorrelated ‘Urban Micro’ channel, as shown in Fig. 7(b).

This can be explained from the design of the algorithm which relies on the parameter l . Peng [21] has suggested that $l = 10$ is the optimal distance in ‘Channel E’ but for the case of ‘Urban Micro’, the optimal length, $l = 10$ no longer valid since the spatial correlation requirement changes according to different type of channel. Other than that, DSA-Scheme 5 sacrifices greater degrees from the selection of the best available subcarrier in preference for avoiding allocation of the same or nearby subcarriers on different spatial subchannels, which depends on the size of l . In other words, there is a trade-off between mitigating self-interference and achieving diversity gain in DSA-Scheme 5. This is shown in Fig. 7(b), where BER curves for DSA-Scheme 5 experience error floor, while interference-aware allocation offered higher BER gain compared to DSA-Scheme 5 as the modulation order and spatial correlation increased for both types of channel model.

The dynamic combination between SINR metric in parallel channels and channel gain metric at spatial interferers makes the interference-aware subcarrier allocation an attractive candidate to combat the debilitating effect of self-interference, compared to the ‘DSA-Scheme 1’ scheme.

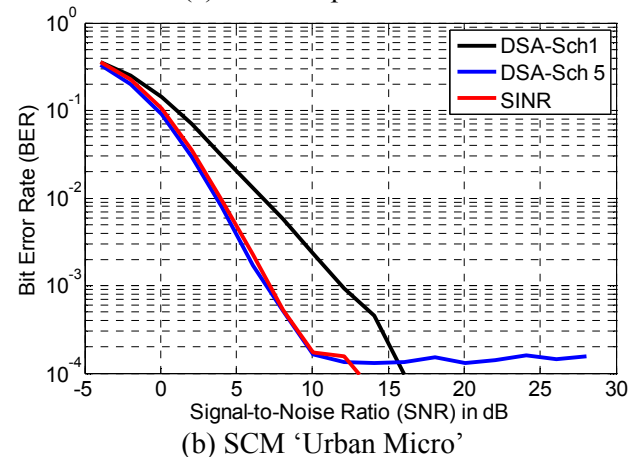
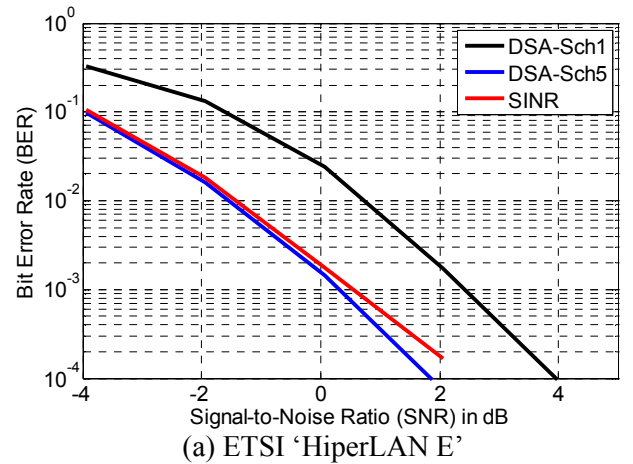


Fig. 6: BER comparison in uncorrelated channels

This can be explained by observing the allocated subcarriers for a user, at a particular time sample in a fully correlated channel between one of the parallel channels and its adjacent spatial interferer, as shown in Fig. 8. In ‘DSA-Scheme 1’, the allocated subcarriers at the spatial interferer are almost the same as to those allocated in the parallel channel (source), which causes the scheme to be unable to differentiate between subcarriers that are severely affected by self-interference and those subcarriers that still can offer good channel quality in a fully correlated channel.

In the interference-aware allocation scheme, the SINR metric at the parallel channel avoids the allocation of similar subcarriers that are affected by self-interference while not compromising the best channel quality given from the channel gain metric at the interfering channel. This results in improved BER performance, as shown in both Fig. 6 and Fig. 7. Other than that, the interference-aware allocation scheme has lower complexity compared to the ‘DSA-Scheme 5’ scheme, since it only uses the spatial parallel subchannels to determine the self-interference caused by the spatial interferers, while the ‘DSA-Scheme 5’ needs to perform the iteration at every spatial subchannel to consider the

previously allocated subcarrier at the previous spatial subchannels. In other words, interference-aware allocation offers lower allocation complexity with extra BER gain compared to ‘DSA-Scheme 5’.

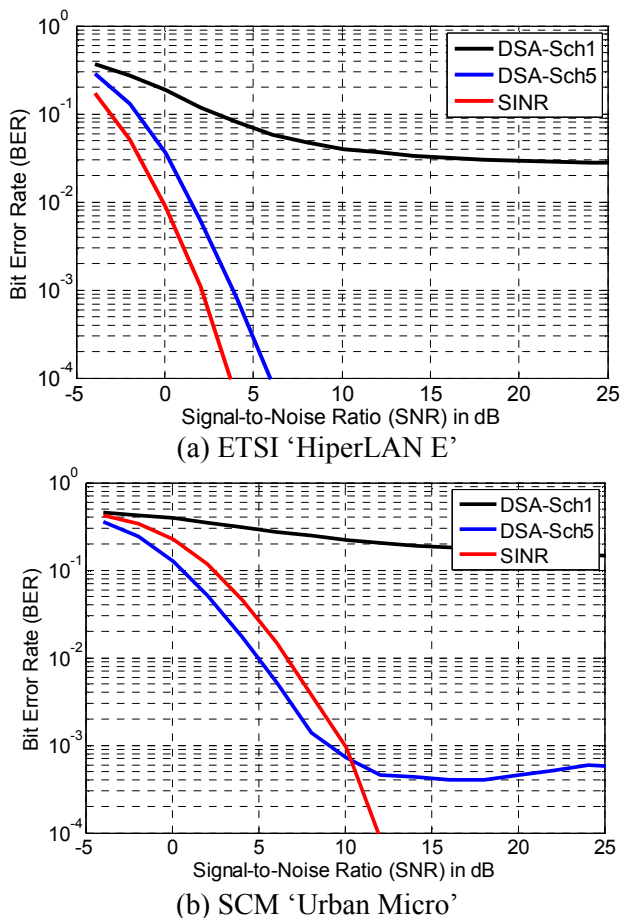


Fig. 7: BER comparison in fully correlated channels

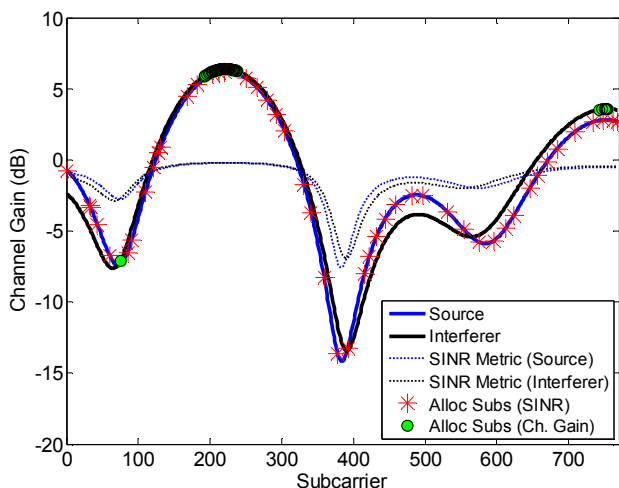


Fig. 8: Example of subcarrier allocation in a ‘Fully’ correlated channel

6 Conclusions

This paper addresses the problem of SM downlink transmission over spatially correlated fading channels from the aspect of subcarrier allocation. From the numerical simulations and analysis, the proposed interference-aware subcarrier allocation has shown to offer low complexity and to achieve substantial BER gains when operating under diverse spatial correlation cases.

As the spatial correlation increased in the channel, the allocation schemes were shown to reduce the effect of self-interference, particularly interference-aware allocation, which had superior BER performance compared to the other considered allocation schemes, namely DSA-Scheme 1 and DSA-Scheme 5. Error analysis also revealed the limitation of DSA-Scheme 5 in mitigating the effect of self-interference. The unit of separation on the next subcarrier parameter, denoted by l , is not flexible and unable to adapt to different type correlation cases and channel model types.

In general, it can be concluded that the proposed algorithm contributes towards the goal of achieving high-speed, yet reliable SM transmission for future wireless networks.

Acknowledgement

The author would like to thanks Universiti Kebangsaan Malaysia for their financial support, under grant scheme number UKM-GGPM-ICT-032-2011.

References:

- [1] S. Alamouti, “A simple transmit diversity technique for wireless communications”, *IEEE Journal on Selected Areas in Communications (JSAC)*, Vol. 16, No. 8, pp. 1451-1458, Oct. 1998.
- [2] G.J. Foschini, G.D. Golden, R.A. Valenzuela, and P.W. Wolniansky, “Simplified Processing for High Spectral Efficiency Wireless Communication Employing Multi-Element Arrays”, *IEEE Transactions on Selected Areas in Communications*, Vol. 17, No. 11, pp. 1841-1852, Nov. 1999.
- [3] G.D. Golden, G.J. Foschini, R.A. Valenzuela, and P.W. Wolniansky. “Detection algorithm and initial laboratory results using the V-BLAST space-time communication architecture”, *Electronics Letters*, Vol. 35, No. 1, pp. 14-15, Jan. 1999.
- [4] D. Gesbert, M. Shafi, D.S Shiu, P.J. Smith, and A. Naguib. “From theory to practice: an overview of MIMO space-time coded wireless

- systems”, Tutorial paper. *IEEE Journal on Selected Areas in Communications (JSAC)*, Vol. 21, No. 3, pp. 281-302, Apr. 2003.
- [5] W. Lee, "Effects on Correlation between Two Mobile Radio Base-Station Antennas," *IEEE Transactions on Communications*, Vol.21, No.11, pp. 1214-1224, Nov 1973.
- [6] P. Kyritsi, D. C. Cox, R. A. Valenzuela, and P. W. Wolniansky, "Correlation analysis based on MIMO channel measurements in an indoor environment", *IEEE Journal on Selected Areas in Communications (JSAC)*, Vol. 21, No. 5, pp. 713-720, June 2003.
- [7] M. Chamchoy, S. Promwong, P. Tangtisanon, J. Takada, "Spatial correlation properties of multiantenna UWB systems for in-home scenarios," *IEEE International Symposium on Communications and Information Technology, 2004. ISCIT 2004*, Vol.2, pp. 1029-1032, Oct. 2004.
- [8] D.-S. Shiu, G. J. Foschini, M. J. Gans, and J. M. Kahn, "Fading correlation and its effect on the capacity of multielement antenna systems," *IEEE Transactions on Selected Areas in Communications*, Vol. 48, No. 3, Mar. 2000.
- [9] A. Intarapanich, P. L. Kafle, R. J. Davies, A. B. Sesay, and J. McRory, "Spatial correlation measurements for broadband MIMO wireless channels," *IEEE 60th Vehicular Technology Conference, 2004. VTC2004-Fall*, Vol.1, pp. 52-56, Sept. 2004.
- [10] G. J. Foschini, "Layered Space-Time Architecture for Wireless Communication in a Fading Environment when Using Multielement Antennas," *Bell Labs Tech. Journal*, pp. 41-59, Autumn 1996.
- [11] C.C. Martin, J.H. Winters, and N.S. Sollenberger, "Multiple-Input Multiple-Output (MIMO) Radio Channel Measurements," *IEEE VTC'2000 Fall Conference*, Sept. 24-28 2000, Boston, USA.
- [12] Jakes, W.C. Jr., *Microwave Mobile Communications*, John Wiley and Sons, New York, 1974.
- [13] S. Catreux, P. F. Driessen, and L. J. Greenstein, "Attainable throughput of an interference-limited multiple-input multiple-output (MIMO) cellular system," *IEEE Transactions on Communications*, Vol. 49, No. 8, pp. 1307-1311, Aug. 2001.
- [14] D. Chizhik, G.J. Foschini, M.J. Gans, R.A. Valenzuela, "Keyholes, correlations and capacities of multi-element transmit and receive antennas", *IEEE 53rd Vehicular Technology Conference, 2001. VTC 2001-Spring*, Vol. 1, pp. 284-287, 2001.
- [15] R.R. Ramirez and F. De Flaviis, "A mutual coupling study of linear and circular polarized microstrip antennas for diversity wireless systems", *IEEE Transactions on Antennas and Propagation*, Vol. 51, No. 2, pp. 238-248, Feb. 2003.
- [16] M.T. Ivrlac, W. Utschick, J.A. Nossek, "Fading correlations in wireless MIMO communication systems", *IEEE Journal on Selected Areas in Communications*, Vol. 21, No. 5, pp. 819- 828, June 2003.
- [17] D. Gore, R. Heath, A. Paulraj, "Statistical antenna selection for spatial multiplexing systems", *IEEE International Conference on Communications, 2002. ICC 2002*, Vol. 1, pp.450-454, May 2002.
- [18] J. Akhtar, D. Gesbert, "A closed-form precoder for spatial multiplexing over correlated MIMO channels", *IEEE Global Telecommunications Conference, 2003. GLOBECOM '03*, Vol. 4, pp. 1847-1851, Dec. 2003.
- [19] K.E. Yong and C. Joohwan, "Random beamforming in MIMO systems exploiting efficient multiuser diversity", in *IEEE 61st Vehicular Technology Conference, 2005. VTC 2005-Spring*. 2005, Vol. 1, pp. 202-205, May 2005.
- [20] A. Doufexi and S. Armour, "Design Considerations and Physical Layer Performance Results for a 4G OFDMA System Employing Dynamic Subcarrier Allocation", *IEEE 16th International Symposium on Personal, Indoor and Mobile Radio Communications, 2005. PIMRC 2005*, Vol. 1, pp. 357-361, Sept. 2005.
- [21] Y. Peng. "Dynamic Sub-carrier Allocation in MIMO-OFDMA Systems". Ph.D. dissertation, University of Bristol, UK, Aug. 2006.
- [22] J. Medbo and P. Schramm, "Channel Models for HIPERLAN/2," ETSI/BRAN document no. 3ERI085B, 1998.
- [23] 3GPP, "Spatial channel model for MIMO simulations", TR 25.996 V7.0.0, 3GPP, 2007. [Online]. Available: <http://www.3gpp.org/>
- [24] S.L. Loyka, "Channel capacity of MIMO architecture using the exponential correlation matrix," *IEEE Communications Letters*, Vol.5, No.9, pp. 369-371, Sep 2001.
- [25] K.I. Pedersen, P.E. Mogensen, B.H. Fleury, "Spatial Channel Characteristics in Outdoor

Environments and Their Impact on BS antenna System Performance”, *IEEE Proc. Vehicular Technology Conference. VTC '98*, Vol. 2, pp. 719-724, May 1998.

- [26] K.I. Pedersen, P.E. Mogensen, B.H. Fleury, “Power Azimuth Spectrum in Outdoor Environments”, *IEEE Electronics Letters*, Vol. 33, No. 18, pp. 1583-1584, Aug. 1997.
- [27] U. Martin, “A Directional Radio Channel Model for Densely Built-up Urban Areas”, *Proc. on 2nd European Personal Mobile Radio Conference. EPMCC '97*, pp. 237-244, Oct. 1997.



Rosdiadee Nordin received his B.Eng. from Universiti Kebangsaan Malaysia in 2001 and Ph.D. from University of Bristol, United Kingdom in 2011. He is currently a lecturer in Department of Electrical, Electronics and System Engineering in Universiti Kebangsaan Malaysia. His

research interests include Multiple-Input Multiple-Output (MIMO), Orthogonal Frequency-Division Multiple Access (OFDMA), resource allocation, green radio, intercell interference, cooperative diversity and indoor wireless localization.